LCTp1-13L
Late-News Paper

Liquid Crystal Iris Realized Using Polymer Gravel Microstructures

Che Ju Hsu [1], Sonam Sharma [2], Rajiv Manohar [2], Chi Yen Huang [3]

Correspondence e-mail: windtrace@nuu.edu.tw
[1]Department of Electro-Optical Engineering, National United University, Miao-Li 360, Taiwan
[2]Liquid Crystal Research Laboratory, Department of Physics, University of Lucknow, Lucknow, Uttar Pradesh 226007, India
[3] Graduate Institute of Photonics, National Changhua University of Education, Changhua 500, Taiwan

Keywords: Liquid crystal, iris, polymer gravel.

ABSTRACT

We present a liquid crystal (LC) iris based on self-assembled polymer microstructures, utilizing a vertically aligned twisted LC cell with a radial gradient in pretilt angles, positioned between crossed polarizers. This configuration enables electrically tunable aperture control with low operating voltage and high aperture tuning ratio, and simplified fabrication.

1 Introduction

An iris is an optical device used to regulate the diameter of a light beam by adjusting the size of its aperture, thereby controlling image quality, resolution, and brightness without altering light intensity. Traditionally, irises employed mechanically operated blades to vary aperture size, offering basic light control but limited by slower response times and reduced precision. Advancements in actuation technologies have led to the development of adaptive irises utilizing mechanisms such as electrowetting, dielectrophoresis, and piezoelectric actuation [1]. Among these, electrowetting and dielectrophoresis are especially promising due to their ability to control liquid droplets with direct voltage input, enabling precise aperture modulation. However, they face challenges such as complex fabrication, limited aperture tunability, and environmental sensitivity. High operating voltages can charge the dielectric liquids or insulating layers, leading to issues like reduced responsiveness and long-term instability [2].

Liquid crystals (LCs), which exhibit both fluid and solid-like properties, offer a compelling alternative. Their optical behavior—such as transmission and scattering—can be finely tuned in response to electrical or mechanical stimuli. This makes LCs ideal for use in displays and adaptive optical components. Their controllable molecular alignment provides precise optical modulation, positioning them as strong candidates for adaptive iris systems. Several LC-based irises have been proposed, including designs utilizing polymer-dispersed LCs with concentric-ring electrode [3], photoconductive layer [4], and twisted LCs integrated with hole-patterned electrodes [5]. However, these approaches present limitations. Polymer-dispersed LCs require high driving voltages due to strong anchoring at droplet interfaces. Implementing photoconductive film-based systems is particularly complex, requiring precise UV illumination via an optical fiber alongside applied voltage. Moreover, LC alignment on photoconductive layers can degrade at increased temperatures due to thermally-induced anchoring transitions. The hole-patterned electrode configuration suffers from weak electric fields at the aperture center.

In our recent researches, a technique has been developed to control pretilt angle of LCs via incorporating a photocurable prepolymer into vertically-aligned LCs [6]. During UV curing, the prepolymer undergoes isotropic vertical phase separation, diffusing toward and then polymerizing on the substrate surfaces. This results in the formation of self-assembled polymer gravel microstructures on the substrate surfaces, which further modify surface polarity so that change the LC pretilt angle. The mechanism behind this polymer microstructure formation has been extensively studied [7], revealing that it arises from surface tension interactions among the LC, prepolymer, and substrate. These polymer gravel arrays align along the rubbing direction, and their structural characteristics—such as amplitude and pitch—can be finely tuned by adjusting the UV curing intensity and the curing voltage. Afterwards, the curing process is carried out through a radial variable neutral density (RVND) photomask, resulting in radial gradient gravel amplitude produced on the substrates. That induces a gradient pretilt angle of LCs, enabling a low voltage LC lens [8].

In this work, we present an adaptive LC iris achieved by incorporating the photocurable prepolymer NOA65 into vertically-aligned twisted LCs. Upon UV curing through a radial variable neutral density (RVND) photomask, the self-assembled polymer gravel microstructures form on the substrates, exhibiting a radial gradient in amplitude. This gradient induces a radial variation in the LC pretilt angles within the twisted configuration. When an external voltage is supplied, LC molecules at the border of the cured region reorient perpendicular to substrate, while those at the center

remain homogeneously aligned. As the voltage increases, this vertical reorientation gradually expands toward the center of the cured region. The LC cell sandwiched between crossed polarizers enables an optical switching effect in the cured regions, resulting in an iris-like behavior. The aperture of the adaptive LC iris can be fully closed at an operating voltage of just 20 V. Compared to conventional adaptive irises based on polymer-dispersed LCs or hole-patterned electrode, the proposed design offers the advantages of simplified fabrication and significantly lower operating voltage.

2. Materials and Methods

An empty LC cell was assembled using two indium–tin–oxide (ITO) glass substrates, each coated with a homeotropic alignment layer of polyimide AL-8088C (Daily Polymer, Taiwan). The substrates were rubbed in orthogonal directions to establish a twisted nematic configuration. The cell gap was maintained using Mylar spacers sandwiched between two substrates, and the gap value was calculated ~ 13 µm using the peak-to-peak technique [9]. The mixture was prepared by combining nematic LC E7 and photocurable prepolymer NOA65 (Norland Optical Adhesive, USA) at a weight ratio of 97.5:2.5. This LC mixture was then injected into the assembled empty cell via capillary action. Initially, the LC molecules were homeotropically aligned, and the NOA65 prepolymer was uniformly dispersed within the LC layer. UV curing was performed using a collimated UV light source (intensity: 5 mW/cm², duration: 3.5 minutes) through a RVND photomask with a diameter of 3.5 mm. During UV exposure, vertical phase separation facilitated the prepolymers to diffuse toward and polymerize on the substrates, forming polymer gravel microstructures with a radial gradient in amplitude. These microstructures induced a corresponding radial gradient in LC pretilt angles within the twisted configuration, as illustrated in Fig. 1(a). The cured LC cell was placed between crossed polarizers, with each polarizer's transmission axis aligned parallel to the rubbing direction of the adjacent substrate. At zero voltage, the twisted nematic configuration rotates the polarization of incident light, allowing it to pass through the analyzer and rendering the cured region optically transparent (Fig. 1(b)). Upon applying a voltage, LC molecules near the border of the cured region—with higher pretilt angles—began to reorient perpendicular to substrates, disrupting the polarization rotation effect. Light passing through these regions retained its original polarization and was blocked by the analyzer (Fig. 1(c)). As the voltage further increased, the vertical reorientation progressed inward, gradually narrowed the aperture. At sufficiently high voltage, the entire cured region transitioned to homeotropic alignment, completely blocking the transmitted light and closing the aperture. In this study, the LC iris was driven using a 1 kHz square-wave AC signal at varying root mean square (RMS) voltages.

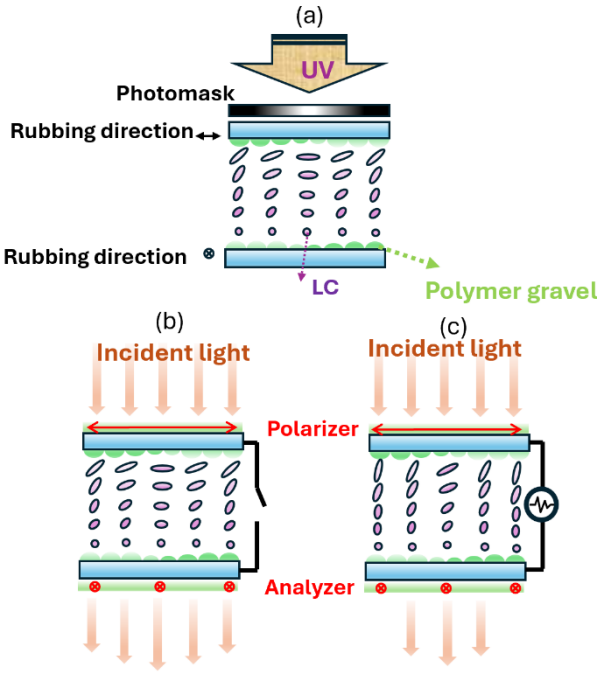

Fig. 1 (a) Cured LC cell through an RVND photomask. Under (b) absence and (c) application of voltage, the light passing through the LC cell placed between the crossed polarizers.

3. Results and Discussion

In a homogeneous LC cell, the alignment of LC directors is parallel to the substrates. This configuration causes the residual phase retardation from the boundary layers, where LC molecules are strongly anchored and difficult to reorient, leading to a higher dark-state voltage. In contrast, a 90° twisted nematic (TN) cell has orthogonal alignment near the substrates. Under high voltage, the residual phase retardations from the two boundaries tend to cancel each other (self-phase compensation), resulting in a lower dark-state voltage [10]. Consequently, the TN configuration is selected for fabricating the adjustable aperture LC iris, as it offers the potential for complete aperture closure with lower power consumption. A simplified experimental setup used to evaluate the performance of the adaptive LC iris. A He-Ne laser (λ = 632.8 nm) was expanded to a 1 cm beam diameter using a beam expander and directed normally onto the LC iris sample. The transmission axes of the polarizer and analyzer were oriented along the rubbing directions of the top and bottom substrates, respectively. A CCD camera attached with a lens module was placed behind the analyzer to observe the output beam's spot image. Figs. 2(a)–2(d) illustrate the aperture modulation of the LC iris under varying applied voltages. Below 4 V, the bright spot diameter remains nearly unchanged, and interference fringes appear due to the gradient in LC pretilt angle, preventing effective iris behavior. At 4 V, the

fringes vanish, revealing a bright spot with a maximum diameter of approximately 3.5 mm [Fig. 2(a)]. The surrounding region remains dark due to homeotropic alignment in non-polymerized area. As the voltage increases to 10 V, the spot diameter reduces to ~2.9 mm [Fig. 2(b)] as border LCs align vertically and block the transmitted light. At 16 V, it decreases further to ~1.8 mm [Fig. 2(c)]. Finally, when the voltage reaches 20 V, the bright spot vanishes completely, indicating full aperture closure [Fig. 2(d)]. These results confirm that the adaptive LC iris capable of complete closure. To quantify the relationship between applied voltage and aperture modulation of the LC iris, the aperture diameter as a function of voltage is plotted in Fig. 2(f). For voltages below 16 V, the aperture diameter decreases approximately linearly with increasing voltage.

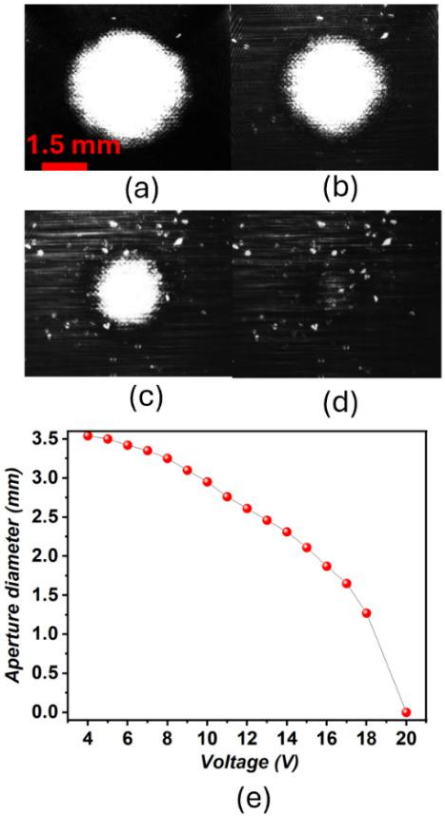

Fig. 2 Output spot diameter of the LC iris under applied voltages of (a) 4 V, (b) 10 V, (c) 16 V, and (d) 20 V. (e) Voltage-dependent variation of the output spot diameter.

The aperture tuning ratio (ATR), commonly used to evaluate the tuning capability of adaptive irises, is defined as

$$\mathrm{ATR} = \left(1 - \frac{A_0}{A}\right), \quad (1)$$

where A and A_o are the maximal and minimal aperture diameters, respectively. By definition, the ATR is always less than or equal to 1. Compared to liquid-based irises, which typically exhibit ATR values between 0.6 and 0.9 [11, 12], the presented LC iris achieves a higher performance, reaching an ATR of 1.

The image performance of the proposed LC iris was demonstrated using the setup shown in Fig. 3(a). The LC cell was placed between crossed polarizers to function as an adaptive iris, with the transmission axes of the polarizer and analyzer aligned parallel to the rubbing directions of the LC cell's top and bottom substrates, respectively. A cardboard placed 24 cm behind the LC cell served as the observed object, while a CCD camera was positioned 8 cm in front of the analyzer to capture the object's image. Figs. 3(b)–3(e) illustrate that the field of view gradually decreases with increasing applied voltage. At an applied voltage of 20 V, the aperture closes completely, effectively blocking the image.

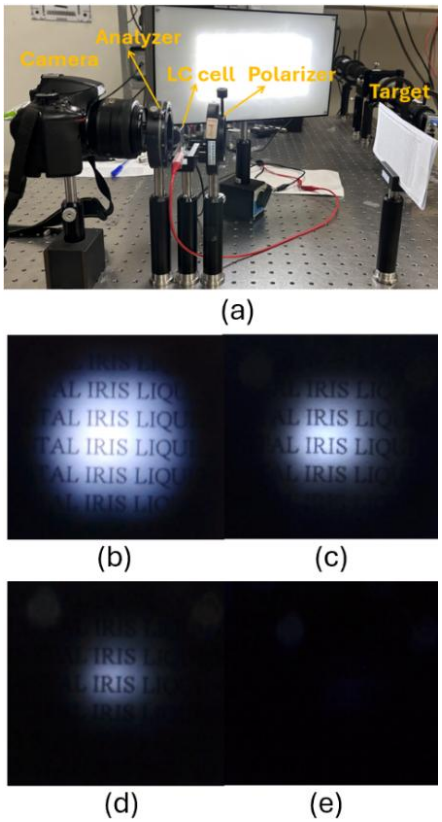

Fig. 3 (a) Experimental setup for evaluating the imaging performance of the proposed LC iris. Captured images of the object through the iris at applied voltages of (b) 4 V, (c) 10 V, (d) 16 V, and (e) 20 V.

To assess the dynamic response of the proposed LC iris, the time-dependent light intensity at the center of the aperture was measured under varying applied voltages. The voltage was increased from 4 V to 20 V for the turn-on process and decreased from 20 V to 4 V for the turn-off process. The turn-on time is defined as the duration during which the transmission drops from its maximum

to minimum value, while the turn-off time corresponds to the increase from minimum back to maximum transmission. Experimental results show a turn-on time of ~17 ms and a turn-off time of ~204 ms. To assess the light transmittance of the open aperture, an expanded He-Ne laser beam with a diameter smaller than 3.5 mm was directed onto the LC iris, which was operated at 4 V. A photodiode placed behind the cell measured the transmitted optical power. With the LC iris installed, the transmitted power registered around 5.7 μW. For comparison, the LC iris was removed, and the same beam was sent directly to the photodiode, resulting in a transmitted power of ~ 16.3 μW. The open aperture's transmittance was calculated to be ~ 35%. The transmittance lower than 50% is mainly due to absorption losses in the polarizer.

4. Conclusions

In this study, we demonstrated an adaptive iris based on twisted LCs and self-assembled polymer gravel microstructures. The proposed approach offers a straightforward fabrication process and allows flexible control over aperture size. By utilizing photo-polymerization through an RVND photomask, a radial gradient in LC pretilt angles was achieved, enabling the voltage-dependent modulation of light transmission. When placed between crossed polarizers, the LC cell exhibited dynamic iris-like behavior, with the aperture gradually closing as the applied voltage increased. The device achieves a high aperture tuning ratio while operating at significantly lower voltages than conventional liquid-based iris.

References

1. S. Schuhladen, F. Preller, R. Rix, S. Petsch, R. Zentel, and H. Zappe, "Iris-like tunable aperture employing liquid-crystal elastomers," J. Adv. Mater. **26**, 7247–7251 (2014).
2. B. Raj, M. Dhindsa, N. R. Smith, R. Laughlin, and J. Heikenfeld, "Ion and liquid dependent dielectric failure in electrowetting systems," Langmuir **25**, 12387–12392 (2009).
3. T.-C. Hsu, C.-H. Lu, Y.-T. Huang, W.-P. Shih, and W.-S. Chen, "Concentric polymer-dispersed liquid crystal rings for light intensity modulation," Sens. Actuators A: Phys. **169**, 341–346 (2011).
4. A. Y.-G. Fuh, K.-N. Chen, and S.-T. Wu, "Smart electro-optical iris diaphragm based on liquid crystal film coating with photoconductive polymer of poly (N-vinylcarbazole)," Appl. Opt. **55**, 6034–6039 (2016).
5. Z. Zhou, H. Ren, and C. Nah, "Adaptive liquid crystal iris," Jpn. J. Appl. Phys. **53**, 092201 (2014).
6. C.-J. Hsu, B.-L. Chen, and C.-Y. Huang, "Controlling liquid crystal pretilt angle with photocurable prepolymer and vertically aligned substrate," Opt. Express **24**, 1463–1471 (2016).
7. C.-J. Hsu, Z.-Y. Cui, C.-C. Chiu, F.-L. Hsiao, and C.-Y. Huang, "Self-assembled polymer gravel array in prepolymer-doped nematic liquid crystals," Opt. Mater. Express **7**, 4374–4385 (2017).
8. C.-J. Hsu, P. Selvaraj, and C.-Y. Huang, "Low-voltage tunable liquid crystal lens fabricated with self-assembled polymer gravel arrays," Opt. Express **28**, 6582–6593 (2020).
9. J. S. Gwag, M. J. Jung, J. C. Kim, and T.-H. Yoon, "Cell Gap Measurement Method for Reflective Liquid Crystal Displays," Jpn. J. Appl. Phys. **43**, L1261 (2004).
10. Y.-q. Lu, F. Du, Y.-H. Lin, and S.-T. Wu, "Variable optical attenuator based on polymer stabilized twisted nematic liquid crystal," Opt. Express **12**, 1221–1227 (2004).
11. M. Xu, H. Ren, and Y.-H. Lin, "Electrically actuated liquid iris," Opt. Lett. **40**, 831–834 (2015).
12. L. Li, C. Liu, H. Ren, and Q.-H. Wang, "Adaptive liquid iris based on electrowetting," Opt. Lett. **38**, 2336–2338 (2013).